IEICE Proceeding Series

Sensitivity of multi-nodal networks consisting of mutually coupled semiconductor lasers

Michail Bourmpos, Apostolos Argyris, Dimitris Syvridis

Vol. 1 pp. 387-390
Publication Date: 2014/03/17
Online ISSN: 2188-5079

2012 International Symposium on Nonlinear Theory and its Applications
NOLTA2012, Palma, Majorca, Spain, October 22-26, 2012

Sensitivity of multi-nodal networks consisting of mutually coupled semiconductor lasers

Michail Bourmpos, Apostolos Argyris and Dimitris Syvridis

Department of Informatics and Telecommunications,
National and Kapodistrian University of Athens,
Panepistimiopolis, Ilisia, 15784, Greece
Email: mmpour@di.uoa.gr, argiris@di.uoa.gr, dsyvridi@di.uoa.gr

Abstract– In this work several multi-nodal all-optical network topologies, based on mutually coupled semiconductor lasers, are investigated regarding synchronization and sensitivity. A sufficient number of such laser nodes with appropriate mutual couplings can result in a collective and synchronized behavior, producing different types of dynamics depending on the network configuration and node parameters. The use of such networks in real world applications is a topic of ongoing investigation. Different topologies are evaluated in terms of sensitivity when specific alterations occur in the network, in order to conclude to the most efficient scheme for sensing applications, intrusion detection or network integrity.

Keywords: Chaos synchronization, mutual coupling, network synchronization, semiconductor lasers.

1. Introduction

Complex dynamics in networks of coupled oscillators have been of great interest over the past decades [1,2]. The nodes in such networks generate signals (as the width swing of a pendulum, the voltage output from an electronic circuit or the optical power of a photonic device) with various dynamics, depending on the non-linearity of the oscillator, as well as on the environmental conditions, the topology of the network and the coupling scheme. The stability of these networks has also been a matter of research in the past few years [3-5].

Semiconductor lasers (SLs), among others, have been proposed as the non-linear elements that compose the nodes in several studies on the aforementioned networks [6,7]. SLs can produce signals with different types of dynamics, from constant wave (CW), to periodic or even chaotic. Each of the above operations has been exploited in real world applications; in particular, synchronized SLs [8] emitting chaotic optical signals have been used in secure communications [9] and cryptography [10].

In our work several network topologies are adopted, consisting of a sufficiently large population of SLs, capable to produce efficient synchrony of the optical signals emitted, as discussed in [11]. Strong optical injection and asymmetric mutual couplings are used in some of the topologies. The latter allows the increase of optical injection between SLs, while preserving the level of injected optical power within reasonable values in cases of nodes receiving accumulated strong injection (central node in a star network). Although intrinsic laser characteristics are selected to be identical in our simulations, different laser operational frequencies were assumed in terms of detuning values from a reference frequency ω_0.

2. Model

A vector formulation of the rate equation mathematical model is used to describe the operation and dynamics of the nodes, which can be applied to any of the investigated network topologies. This model is based on the Lang Kobayashi rate equation model [12], originating from the representation used in [13] and including frequency detuning terms as in [11].

$$\frac{dE(t)}{dt} = i\Delta\omega \circ E(t) + \frac{1}{2}(1+ia)\left(G(t) - \frac{1}{t_{ph}}\right) \circ E(t) + K^T(E(t-\tau)) \circ e^{-i\omega_0\tau}) + \sqrt{D}\xi(t) \quad (1)$$

$$\frac{dN(t)}{dt} = \frac{I}{e} - \frac{N(t)}{t_s} - G(t) \circ |E(t)|^2 \quad (2)$$

$$G(t) = g_n(N(t) - N_0) \circ (1 + s|E(t)|^2)^{\circ -1} \quad (3)$$

$E(t)=[E_1(t)\ E_2(t)\ \ldots\ E_n(t)]$ and $N(t)=[N_1(t)\ N_2(t)\ \ldots\ N_n(t)]$ are the vectors of the SLs optical fields and carrier densities respectively. $\xi(t)$ is the vector of uncorrelated complex Gaussian white noises. The time delays and couplings between the nodes of the network are kept in the nxn arrays K and τ, where the actual values from node i to node j are represented as τ_{ij} and K_{ij} respectively. By appropriate manipulation of the coupling and time delay arrays (K and τ) we can construct the desired network topologies, adopting coupling asymmetries wherever needed. The result of the Hadamard product ($\circ$) between the nxn arrays of the time delayed optical field $E(t-\tau)$ and the phase shift $e^{-i\omega_0\tau}$ in equation (1), is also a nxn array, where the element (i,j) is the delayed optical field of i

injected into j followed by the corresponding phase shift, equal to $E_i(t-\tau_{ij})e^{-i\omega_0\tau_{ij}}$.

Vector I of equation (2) contains the biasing current for all lasers which is set to $I=25mA$ throughout this work, while the solitary lasing threshold is $I_{th}=17.4mA$. Each laser is detuned with respect to the reference laser frequency ω_0, at variable values $\Delta\omega_j$, kept in the vector $\Delta\omega$ of equation (1).

Finally, vector $|E(t)|^2 = [|E_1(t)|^2\ |E_2(t)|^2\ \dots\ |E_n(t)|^2\ ]$ contains the power of optical fields and the Hadamard inverse $(1+s|E(t)|^2)^{\circ -1}$ yields $1/(1+s|E_i(t)|^2)$for the i_{th} laser. SLs share the same intrinsic parameter values, so there is no need to write parameters α, t_{ph}, g_n, s, $N0$ in vector form, although this is also possible. The parameter values used in our investigation are as follows:

TABLE 1
INTRINSIC LASER PARAMETERS

α	linewidth enhancement factor	5
t_{ph}	photon lifetime	$2psec$
ω_0	reference laser frequency	$2\cdot\pi\cdot\lambda_0$
λ_0	reference laser wavelength	$1550nm$
D	noise strength	$10^{-5}\ nsec^{-1}$
e	electronic charge	$1.602\cdot10^{-19}$ C
t_s	carrier lifetime	$1.54nsec$
g_n	gain coefficient	$1.2\cdot10^{-5}\ nsec^{-1}$
N_0	carrier density at transparency	$1.25\cdot10^{8}$
s	gain saturation coefficient	$5\cdot10^{-7}$

3. Network Topologies

In all network topologies presented below, we formulate the coupling matrix K and assume that the time delay matrix is similarly constructed, with constant values of $5ns$ delays between the nodes. The frequency detunings from the reference laser frequency are randomly chosen, following a Gaussian distribution in the range of $2\pi\cdot(\pm1\text{GHz})$.

3.1. Star Network

For a star network of 50 remote nodes coupled through a central typical SL we formulate the 51x51 coupling matrix K as follows:

$$K=\begin{bmatrix} 0 & 0 & \dots & 0 & k_{1,51} \\ 0 & 0 & \dots & 0 & k_{2,51} \\ \vdots & \vdots & \vdots & \vdots & \vdots \\ 0 & 0 & \dots & 0 & k_{50,51} \\ k_{51,1} & k_{51,2} & \dots & k_{51,50} & 0 \end{bmatrix} \quad (4)$$

The 51st row of the matrix is matched with the central node of the star topology. We have assumed identical couplings from the hub node to the star nodes ($k_{51,i}=k_{51,j}=k$) and from star nodes to the hub $k_{i,51}=k_{j,51}=\beta\cdot k$, where $0<\beta<1$ is a coupling asymmetry coefficient we have introduced to keep the accumulated optical injection into the hub laser within reasonable range.

We must point out that for this topology the hub laser frequency detuning is assumed to be zero, without loss of generality.

For different values of the parameter pair (k,β), a mapping of the mean zero-lag cross-correlation between all SL pairs (i,j) is constructed, as shown in figure 1.

Based on this mapping, we have selected the pair of parameters $\{k=60ns^{-1}\ ,\ \beta=0.5\}$ where high zero-lag mean cross-correlation is achieved ($C_{i,j}^{mean}=0.921$) in combination with higher complexity [14]. For this pair of values, a sensitivity analysis, when a SL is added or subtracted from the network, is performed.

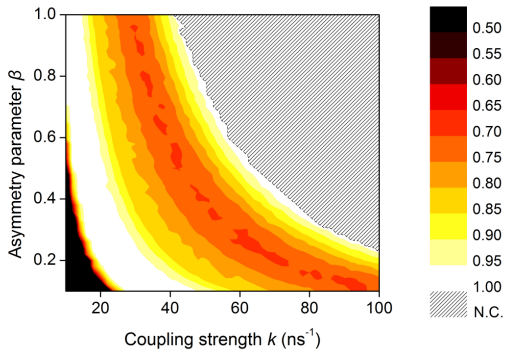

Figure 1. Mean zero-lag cross-correlation among the 50 star lasers.

First we connect a new node to the network, with various coupling and time-delay parameter values. We are interested in whether the connection of this non-identical laser with unmatched operational parameters will influence the behaviour of the backbone network. Moreover, we would like to know the tolerance in the parameter mismatch in order for the SL to be synchronized with the rest of the nodes in the network and if this node-addition can somehow be detected.

For various values in the frequency detuning of the newly connected node and its time delay from the hub laser we calculate the change in the mean and minimum (worst case) zero-lag cross correlation of the original 50-node star network (figure 2).

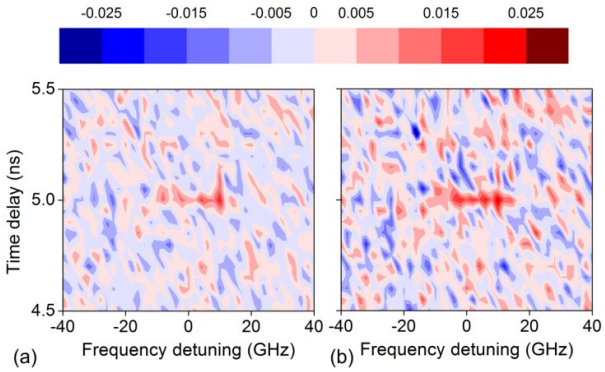

Figure 2. Change in the mean (a) and minimum (b) zero-lag cross correlation of the 50 star laser network, when an additional laser is connected to the network, for various values of frequency detuning and time delay of the added laser.

It is evident that the network has absorbed the mismatch of the one additional laser, even if its detuning is significantly larger than 1GHz or its time-delay is different than *5ns*. The difference in the mean and minimum zero-lag cross-correlation is statistical and calculated to be $|\Delta C_{i,j}^{mean}|$ *~0.013* and $|\Delta C_{i,j}^{min}|$ *~0.021* respectively. The only parameter values of the added node for which the change is not statistical lie in the region of τ*=5ns* and for small frequency detuning values. The consistence of these values with the rest of the network parameters imposes a measurable positive change in the mean correlation value, making the synchronized new node detectable by the network.

The mean value of the maximum cross-correlation - regardless of lag - between the newly connected laser and the 50 SLs in the network is maximized for zero frequency detuning, as shown in figure 3a. Figure 3b shows the time lag for which the maximum cross-correlation between the added node and the rest of the SLs in the network occurs. It is clear that when the time-delay is not *5ns* - as is between all other nodes and the hub - only lagged synchronization is observed.

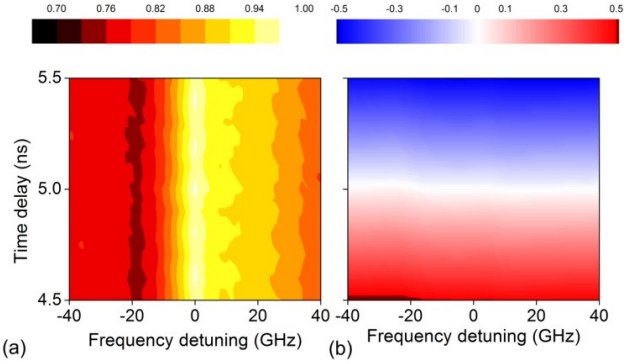

Figure 3. Maximum of the mean cross-correlation (a) and corresponding time lag in ns (b) between the connected laser and the 50 SLs of the star network, for various values of frequency detuning and time delay of the added laser.

Disconnecting a SL from the original network of 50 nodes is a rather more straightforward case. The mean correlation of the network after disconnecting the new laser is shifted now to a lower value by $\Delta C_{i,j}^{mean}$ = *-0.012*, attributed to a reduction of the coupling strength among the 49 lasers left within the network. However, simulation results prove that there is no dependence on the value of the disconnected laser's frequency detuning; the effect of disconnecting a node with large detuning seems almost equivalent to disconnecting a node with close to zero detuning.

3.2. Fully-connected Mesh Network

For a fully-connected mesh network of 50 SLs, each one coupled to every other, we formulate the 50x50 coupling matrix *K* as follows:

$$K = \begin{bmatrix} k_{1,1} & k_{1,2} & \dots & k_{1,49} & k_{1,50} \\ k_{2,1} & k_{2,2} & \dots & k_{2,49} & k_{2,50} \\ \vdots & \vdots & \vdots & \vdots & \vdots \\ k_{49,1} & k_{49,2} & \dots & k_{49,49} & k_{49,50} \\ k_{50,1} & k_{50,2} & \dots & k_{50,49} & k_{50,50} \end{bmatrix} \quad (5)$$

where $k_{i,i}$*=0* for zero feedback of the SL nodes.

Assuming equal couplings $k_{i,j}$*=k*, $\forall i,j$ and for different values of *k* we plot the mean zero-lag cross-correlation between all SL pairs (figure 4). Based on this figure we choose *k=1.5ns*$^{-1}$ as the coupling between the nodes, which yields a mean zero-lag cross-correlation of $C_{i,j}^{mean}$*=0.964* and then add a new node, with different parameter values, to the network.

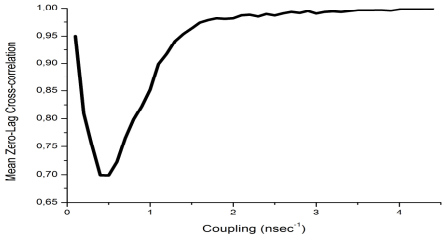

Figure 4. Mean zero-lag cross-correlation among the 50 star lasers.

Again, the network has absorbed the mismatch of the one additional laser (figure 5). The difference in the mean and minimum zero-lag cross-correlation is statistical and calculated to be $|\Delta C_{i,j}^{mean}|$ *~0.001* and $|\Delta C_{i,j}^{min}|$ *~0.004* respectively. The newly added SL produces a consistent, non-statistical increase in the mean and minimum zero-lag cross-correlation of the network, only when it's time-delay is equal to *5ns* - the common time-delay of all nodes - and for small values of frequency detuning. Similar results to those of the star network are obtained for the maximum value of the mean cross-correlation between the connected laser and the 50 SLs in the fully-connected mesh network, as well as for the corresponding time-lag, for various detuning and time delay values of the added node.

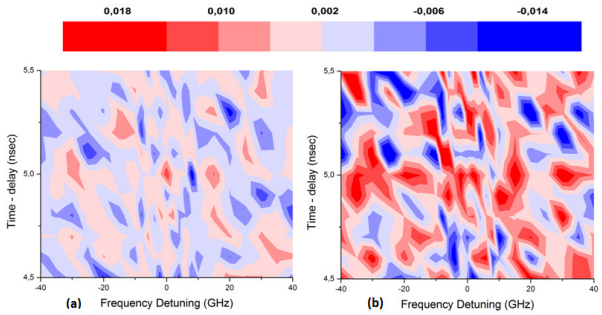

Figure 5. Change in the mean (a) and minimum (b) zero-lag cross correlation of the 50 laser fully-connected mesh network, when an additional laser is connected to the network, for various values of frequency detuning and time delay of the added laser.

Disconnecting a node from the network leads to minor mean cross-correlation degradation, which is statistical and independent of the removed node's frequency detuning, as in the case of the star network.

3.3. Ring Network

For a ring network of 50 SLs, where every node is connected only to its two neighbors, the 50x50 coupling matrix K is formulated as follows:

$$K = \begin{bmatrix} k_{1,1} & k_{1,2} & 0 & \dots & 0 & 0 & k_{1,50} \\ k_{2,1} & k_{2,2} & k_{2,3} & \dots & 0 & 0 & 0 \\ 0 & k_{3,2} & k_{3,3} & \dots & 0 & 0 & 0 \\ \vdots & \vdots & \vdots & \vdots & \vdots & \vdots & \vdots \\ 0 & 0 & 0 & \dots & k_{48,48} & k_{48,49} & 0 \\ 0 & 0 & 0 & \dots & k_{49,48} & k_{49,49} & k_{49,50} \\ k_{50,1} & 0 & 0 & \dots & 0 & k_{50,49} & k_{50,50} \end{bmatrix} \quad (6)$$

with $k_{i,i}=0$ for zero feedback of the SL nodes, common couplings $k_{i,j}=k$, $\forall i,j$ and time delays of *5ns*. The nodes are sorted and positioned in the ring by increasing frequency detuning values.

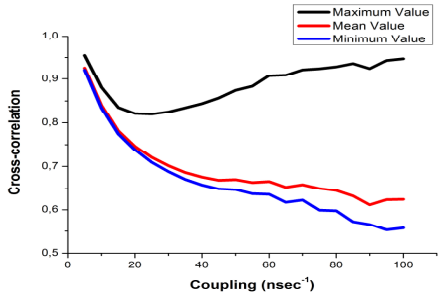

Figure 6. Maximum, mean and minimum cross correlation of all pairs in the 50 node fully-connected mesh network, regardless of lag.

For different coupling values we calculate the maximum cross-correlation between all node-pairs and the corresponding lag. Only the second nearest neighbors (*i-2* and *i+2* for the i^{th} node) have consistently their maximum cross-correlation value at zero lag, even though this is also observed in several other 'even pairs' (j with $j+2\cdot l$). We plot (figure 6) the maximum, mean and minimum of these cross-correlation (regardless of lag) values. Only for small couplings, where low complexity dynamics are observed, we obtain high cross-correlation values. As coupling and consequently complexity increase, cross-correlation monotonically decreases. Figure 7a depicts the deterioration of the maximum cross-correlation - regardless of lag - between node 1 and the rest of the 49 nodes in the network, for coupling $k=50ns^{-1}$, as their neighbouring order increases.

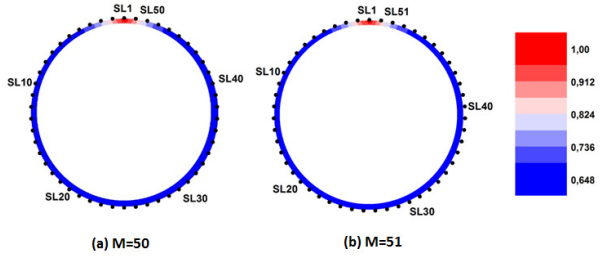

Figure 7. Maximum cross-correlation between SL1 and the rest of the SLs in the network, for $k=50ns^{-1}$ and regardless of time-lag, for (a) 50 SLs and (b) 51 SLs.

Adding a node between the 1st and the 50th node, with time delays of *5ns* and a random negative frequency detuning, forms a new 51-node ring network. The new network has similar maximum cross-correlation values as the previous 50-node network (figure 7b). However, differences between the two networks are evident in the time-lags of maximum cross-correlation between the nodes and therefore in their behaviour (figure 8).

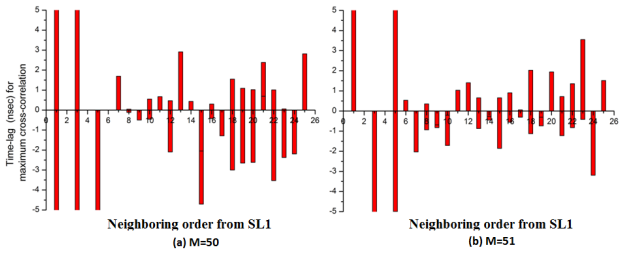

Figure 8. Time-lag of maximum cross-correlation between SL1 and the rest of the nodes in respect to their neighboring order from SL1, for networks of (a) 50 SLs and (b) 51 SLs.

In the case of the 50 node network, the two nodes positioned right next to the reference node (neighboring order is 1), or those at neighboring order of 3, seem to lag and lead the dynamics respectively. For the case of the 51-node network, both nodes at neighboring order of 1 lead the dynamics, while those at neighboring order of 3 lag behind. In both networks, nodes at neighboring orders of 2 or 4 exhibit maximum cross-correlation at zero-lag. Beyond the neighboring order of 4 we have irregular lags and very small cross-correlation values in both networks.

4. Conclusion

We have investigated three different coupled SL network topologies in terms of their sensitivity. Star or fully-connected mesh networks seem to maintain high values of mean zero-lag cross-correlation between all of their nodes, regardless of the characteristics of the node added or removed. Ring networks on the other hand exhibit high cross-correlation only between neighboring nodes. The addition of a node in the ring of SLs alters the network behavior, keeping however cross-correlation values at similar levels. All the above topologies deserve further investigation, as they exhibit behavior that could be exploited in future applications like sensing, intrusion detection or network integrity.

References

[1] S.H. Strogatz, Nature 410, 268-276, 2001.
[2] S. Boccaletti et al., Phys. Rep. 424, 175-308, 2006.
[3] L.M. Pecora and T.L. Caroll, Phys. Rev. Lett. 80, 2109
[4] V. Flunkert et.al., Phys. Rev. Lett. 105, 254101 (2010).
[5] A. Englert et. al., Phys.Rev.E 83, 046222 (2011)
[6] M. Nixon et. al., Phys. Rev. Lett. 108, 214101 (2012).
[7] Thomas Dahms, PhD thesis, TU Berlin, 2011.
[8] L.M. Pecora and T.L. Caroll, Phys.Rev.Lett.,vol.64,821-824, 1990.
[9] A. Argyris et. al., Nature, vol. 438, n. 7066, pp. 343-346, 2005.
[10] A. Uchida, et. al., Nat. Photonics 2(12), 728–732 (2008).
[11] J. Zamora-Munt et.al., Phys. Rev. Lett., vol. 105, 264101, 2010.
[12] R.Lang, K.Kobayashi, IEEE J.Q.E., vol. 16, pp. 347-355, 1980.
[13] I. Fischer et.al., Phys. Rev. Lett., vol. 97, 123902, 2006.
[14] M.Bourmpos et.al., accepted for publication IEEE JLT 2012